PCCP

ROYAL SOCIETY OF CHEMISTRY

PAPER

View Article Online
View Journal | View Issue

Check for updates

Cite this: *Phys. Chem. Chem. Phys.*, 2021, **23**, 26729

Excited-state structure of copper phenanthroline-based photosensitizers†

Alexander Guda,[a] Johannes Windisch,[b] Benjamin Probst,[b] Jeroen A. van Bokhoven,[cd] Roger Alberto,[b] Maarten Nachtegaal,[c] Lin X. Chen[ef] and Grigory Smolentsev*[c]

Received 22nd June 2021,
Accepted 12th November 2021

DOI: 10.1039/d1cp02823e

rsc.li/pccp

Cu diimine complexes present a noble metal free alternative to classical Ru, Re, Ir and Pt based photosensitizers in solution photochemistry, photoelectrochemical or dye-sensitized solar cells. Optimization of these dyes requires understanding of factors governing the key photochemical properties: excited state lifetime and emission quantum yield. The involvement of exciplex formation in the deactivation of the photoexcited state is a key question. We investigate the excited-state structure of $[Cu(dmp)_2]^+$ and $[Cu(dsbtmp)_2]^+$ (dmp = 2,9-dimethyl-1,10-phenanthroline, dsbtmp = 2,9-di-*sec*-butyl-3,4,7,8-tetramethyl-1,10-phenanthroline) using pump–probe X-ray absorption spectroscopy (XAS) and DFT. Features of XAS that distinguish flattened tetrahedral site and 5-coordinated geometry with an additional solvent near Cu(II) center are identified. Pump–probe XAS demonstrates that for both complexes the excited state is 4-coordinated. For $[Cu(dmp)_2]^+$ the exciplex is 0.24 eV higher in energy than the flattened triplet state, therefore it can be involved in deactivation pathways as a non-observable state that forms slower than it decays. For $[Cu(dsbtmp)_2]^+$ the excited-state structure is characterized by Cu–N distances of 1.98 and 2.07 Å and minor distortions, leading to a 3 orders of magnitude longer excited-state lifetime.

Published on 15 November 2021. Downloaded on 12/20/2021 11:28:06 AM.

Introduction

Cu-Based diimine complexes are a low-cost alternative to replace the widely used Ru-polypyridyl photosensitizers in dye-sensitized solar cells (DSSCs), molecular systems for artificial photosynthesis and photoelectrochemical cells due to their similar absorption spectrum and the metal-to-ligand-charge-transfer (MLCT) nature of their excited state.[1–4] Some Cu(I) complexes demonstrate thermally-activated delayed fluorescence (TADF), therefore they are also used as luminophores for organic light-emitting diodes (OLEDs).[5,6] Significant progress has been achieved during the last few years in implementing Cu complexes in different light-driven systems, where they can be used in multicomponent systems for photocatalytic hydrogen evolution,[7–10] for efficient injection of electrons into TiO_2[2,11] mimicking the process in DSSC and for electron donation sites in supramolecular systems.[12,13] It has been found that a better shielding of the formal Cu(II) center in the MLCT state from solvent molecules, mainly by using substituents at the 2,9 positions of phenanthroline, leads to longer excited-state lifetimes.[14,15] Many studies reported on this shielding effect in the past by using structural dependent photoluminescence lifetime and excited-state lifetime measurements.[14,16–18] In particular, for $[Cu(dmp)_2]^+$ (dmp = 2,9-dimethyl-1,10-phenanthroline) an excited state lifetime of 1.7 ns in acetonitrile has been observed.[19] The longest lifetime (2.72 μs in CH_2Cl_2) has been reported for $[Cu(dsbtmp)_2]^+$ (dsbtmp = 2,9-di-*sec*-butyl-3,4,7,8-tetramethyl-1,10-phenanthroline) with bulky *sec*-butyl groups at the 2,9 positions.[20] That work also reported that the substituents at 3,8 positions induce an additional steric hindrance for the *sec*-butyl rearrangement after photoexcitation and therefore further prolong the MLCT state lifetime. A similar long-lived excited state (2.32 μs in CH_2Cl_2) has been observed for $[Cu(diptmp)_2]^+$ (diptmp = 2,9-diisopropyl-3,4,7,8-tetramethyl-1,10-phenanthroline).[21] The reduction of flattening distortions as a result of photoexcitations by introducing a steric hindrance typically increases the energy gap between photoexcited and ground states, which leads to longer excited-state lifetimes. There is a large set of Cu(I) diimine molecules with lifetimes in the nanosecond range, which follows the trend that in the same solvent, the excited state lifetimes are longer for

[a] *The Smart Materials Research Institute, Southern Federal University Rostov-on-Don, 344090, Russia*
[b] *Department of Chemistry, University of Zurich, Zurich, 8057, Switzerland*
[c] *Paul Scherrer Institute, Villigen, 5232, Switzerland. E-mail: grigory.smolentsev@psi.ch*
[d] *Department of Chemistry, ETH Zurich, Zurich 8093, Switzerland*
[e] *Chemical Sciences and Engineering Division, Argonne National Laboratory, Argonne 60439, IL, USA*
[f] *Department of Chemistry, Northwestern University, Evanston 60208, IL, USA*

† Electronic supplementary information (ESI) available. See DOI: 10.1039/d1cp02823e

Published on 15 November 2021. Downloaded on 12/20/2021 11:28:06 AM.

complexes with bulkier ligands at the 2,9 positions of phenanthroline while stronger interacting solvents (*e.g.* acetonitrile) always shorten the excited state lifetime.[14]

Over a decade ago some of us have reported that an exciplex is formed as a result of the interaction of the photoexcited $[Cu(dmp)_2]^+$ (in the triplet state) with a solvent acetonitrile molecule leading to a five-coordinated Cu atom.[22] This result supported the idea of the formation of an exciplex proposed by McMillin.[16] Our result was based on the comparison of experimental pump–probe X-ray absorption near edge structure (XANES) with theoretical spectra calculated for models with different Cu coordination, while McMillin made his suggestion by measuring the emission in the visible range for a series of related Cu complexes in different solvents. After our publication, the first XRD structure of $[Cu^{II}(dmp)_2(CH_3CN)]^{2+}$ was reported.[23] The Cu(II) in this complex forms a short bond (2.01 Å) to acetonitrile. Significant rocking distortions (that change the angle between the C_2 symmetry axes of phenanthrolines, see Fig. 1) opens up space for the solvent molecule to bind directly to Cu(II). In a later study, the photoexcited $[Cu(dbtmp)_2]^+$ (dbtmp = 2,9-di-*n*-butyl-3,4,7,8-tetramethyl-1,10-phenanthroline) has also been investigated with a similar combination of pump–probe XANES and theoretical simulations of spectra.[24] In this case, a four-coordinated model gave better agreement with the experiment, which conforms to the trends described above: long *n*-butyl chains restrict the access of solvents to Cu(II), which makes the excited state lifetime longer.

In 2013, based on the comparison of transient XANES spectra of photoexcited $[Cu(dmp)_2]^+$ in two solvents, classical molecular dynamics and quantum mechanics/molecular mechanics (QM/MM) simulations, it was reported that an exciplex with a short solvent–metal bond is not formed and mainly flattening distortions occur after photoexcitation, keeping the Cu center four-coordinated.[25] Here, the authors explained the difference of excited-state lifetimes in the series of diimine Cu complexes by the variations in the size of the energy gap (within the weak coupling limit, the rate of non-radiative processes decreases exponentially with the increase of the energy gap[26]). Their calculation showed that five complexes followed this trend, but there were three outliers, which may be due to the difference in spin–orbit coupling. The authors proposed that the solvent dependence of the lifetime is due to the differences of electrostatic interactions between the solvent and $[Cu(dmp)_2]^+$ which change the energy gap.

To proceed further in the development of efficient Cu-based photosensitizers, it is crucial to clarify if the formation of an exciplex with a short (<2.3 Å) metal–solvent bond is possible and how this influences the decay of the excited state. This will answer whether the maximization of the energy gap or further shielding of the Cu from solvent molecules should be the main approach to achieve an increase in the excited-state lifetime. To move forwards from the situation where different interpretations[22,25] of similar experimental transient XANES spectra[19,24,25,27,28] have been published, it is important to understand which spectral features can be used to monitor the formation of an exciplex with a short metal–solvent bond and how these spectral features differ from the spectral features of a metal-to-ligand charge transfer state with flattening distortions only. To address this we have considered two compounds (Fig. 1): classical $[Cu(dmp)_2]^+$ which was the subject of previous investigations[22,25] and $[Cu(dsbtmp)_2]^+$ which is the Cu-phenanthroline-based photosensitizer with the longest excited state lifetime reported so far.

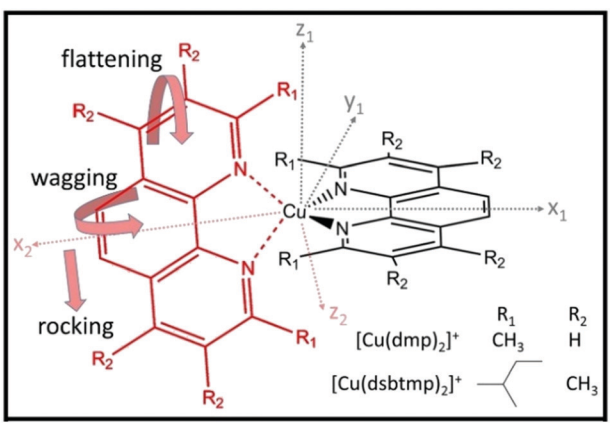

Fig. 1 Different types of structural distortions in Cu photosensitizers with phenanthroline-based ligands. Two orthogonal sets of basis vectors linked to different ligands are shown, where x_1 and x_2 are C_2 symmetry axes of the phenanthrolines, and z_1 and z_2 are perpendicular to the planes of the corresponding phenanthrolines. Rocking distortions changes the angle between z_1 and x_2, flattening changes the angle between z_1 and z_2, and wagging changes the angle between y_1 and x_2.

Results

DFT calculations of excited states

Fig. 2 shows two projections of the potential energy surfaces for $[Cu(dmp)_2]^+$. Ultrafast dynamics, including intersystem crossing, can be well described using the flattening angle as the reaction coordinate. This type of distortion has been studied previously,[14,28–31] in particular, Levi *et al.*[31] found a coupling of the flattering motion with solvent interactions and rotations of methyl groups. The intersystem crossing time is 9–20 ps for $[Cu(dmp)_2]^+$ and 2–6 ps for $[Cu(dsbtmp)_2]^+$.[15] We decided to explore the role of other types of distortions, namely rocking and wagging, on the dynamics observed in the nanosecond range, in particular on the possible formation of the exciplex state. Projections presented at the top of Fig. 2 show that the exciplex is significantly higher in energy than the 4-coordinated triplet state, especially, for relatively small flattening distortions. Nevertheless, after additional relaxation alone rocking distortions, approximately by 20°, this state becomes only 0.24 eV above the equilibrium 4-coordinated MLCT triplet geometry (Fig. 2, bottom). Therefore, the combination of flattening and rocking distortions is important to enabling the interaction of the Cu(II) center of the photoexcited complex with the solvent.

 This journal is © the Owner Societies 2021

Published on 15 November 2021. Downloaded on 12/20/2021 11:28:06 AM.

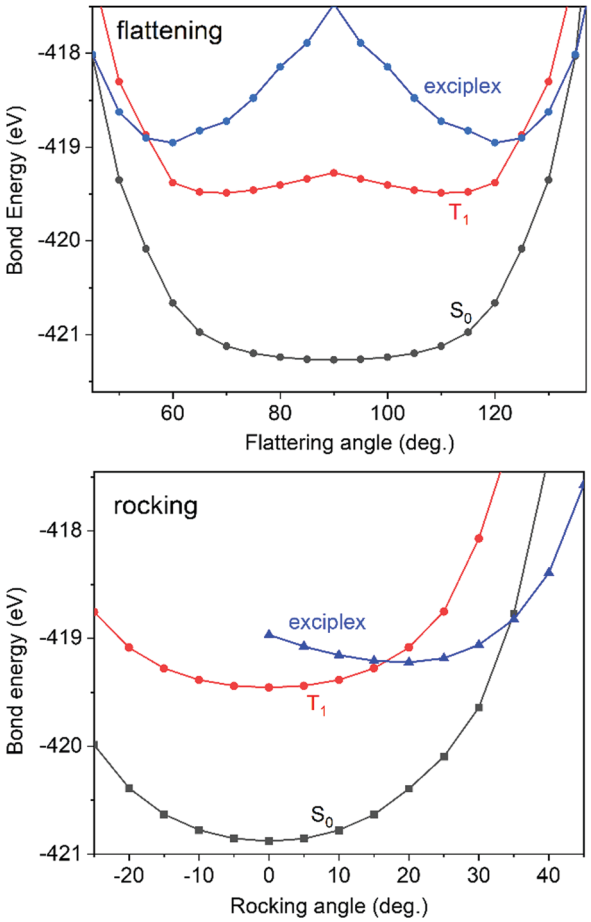

Fig. 2 Cross-sections of the potential energy surfaces for singlet, triplet and exciplex states of the $[Cu(dmp)_2]^+$ molecule. Top panel: Variation of the flattering angle while fixing the rocking angle to 0° as in the DFT optimized triplet structure. Bottom panel: Variation of the rocking angle while fixing the flattering angle to 117° as in the DFT optimized exciplex structure. Cu–N distance in the exciplex is set to 2.33 Å.

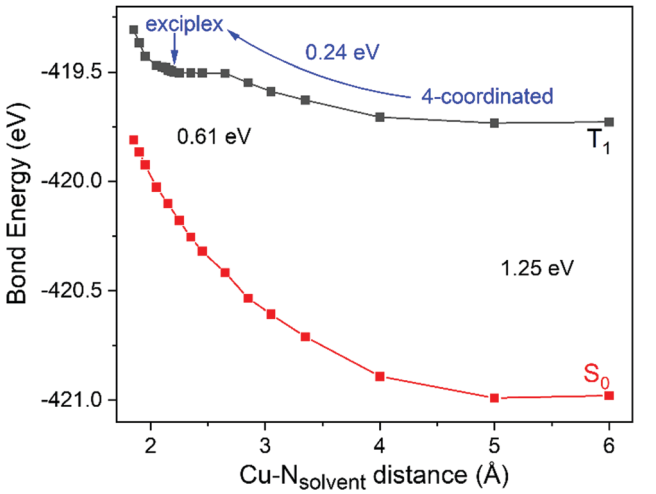

Fig. 3 Energies of the triplet excited state of the $[Cu(dmp)_2]^+$–acetonitrile system (black line) obtained using DFT for relaxed geometries with constrained distances between Cu and acetonitrile are compared with the energies of the singlet ground state corresponding to the same structures.

The role of Cu–solvent distance on the energies of states is explored in Fig. 3. An exciplex with a short metal–solvent bond exists and it is separated from the non-bound structure by 0.24 eV (black curve in Fig. 3). The energy gap between the triplet excited and singlet ground states is small, 0.61 eV, for the geometry of the exciplex (Cu–acetonitrile distance 2.15 Å) in comparison to 1.25 eV for the four-coordinated structures (Cu–acetonitrile distance 5.0 Å). The DFT geometry optimization converged to the energy minimum for exciplex, but the stability of this state is low because: (i) the barrier that separates it from 4-coordinated geometry is low and (ii) in competition with solvent dissociation, the non-radiative decay to the ground state can also occur.

For the $[Cu(dsbtmp)_2]^+$ photosensitizer, it was postulated that *sec*-butyl groups at the 2,9 positions of phenanthroline shield the Cu atom so well that solvent molecules cannot reach the Cu center in the excited state. For this reason, previously reported DFT simulations for the triplet state of this complex were performed starting from this assumption.[20] To check the validity of this assumption, we constructed a five-coordinated model with additional acetonitrile coordinating to Cu and performed the geometrical optimization. The excited-state structure converged to a local energy minimum and the exciplex has MLCT character as seen from the spin density distribution (Fig. S5, ESI†). Analogous results were obtained for $[Cu(dsbtmp)_2]^+$ in dimethylformamide (DMF) solvent (Fig. S5 and S6, ESI†). Both acetonitrile and DMF are coordinating solvents. Gutmann's donor numbers for acetonitrile is 14.1 kcal mol^{-1} and for DMF is 26.6 kcal mol^{-1}, therefore similar coordinating behavior of these two solvents is expected.[32] The experiments, presented in the next sections, were performed for $[Cu(dsbtmp)_2]^+$ in DMF and $[Cu(dmp)_2]^+$ in acetonitrile. To check the difference between these two solvents, the calculations for $[Cu(dsbtmp)_2]^+$ were performed for both of them. The structures are compared in Table S1 (ESI†). We have found that in the structure in acetonitrile, the Cu–solvent distance is 2.07 Å. For such an exciplex structure, the complex distorts along wagging deformation coordinates instead of flattening distortions. Flattening distortions are blocked significantly by the *sec*-butyl groups: from the comparison of Fig. 2 top and Fig. S7 (ESI†) the energy minima for $[Cu(dsbtmp)_2]^+$ are significantly deeper than for $[Cu(dmp)_2]^+$. Wagging deformations make the geometry of five-coordinated Cu close to the D_{3h} instead of T_d symmetry for the four-coordinated complex. The average Cu–N distances of the two ligands are 2.07 Å and 2.24 Å, while the dihedral angle between phenanthroline planes is 96°. Calculations for an alternative four-coordinated geometry of the excited state gave Cu–N bonds to the two ligands of 1.98 Å and 2.07 Å. Thus, our calculations suggest, that for $[Cu(dsbtmp)_2]^+$, despite the bulkiness of the 2,9 substituents, an energetically stable triplet excited state with a short Cu–solvent bond exists, but its energy is higher by 0.73 eV than that of the four-coordinated triplet. While the required energy is available shortly after the photoexcitation, a temperature-activated transition from the relaxed four-coordinated triplet to the five-coordinated state seems

Published on 15 November 2021. Downloaded on 12/20/2021 11:28:06 AM.

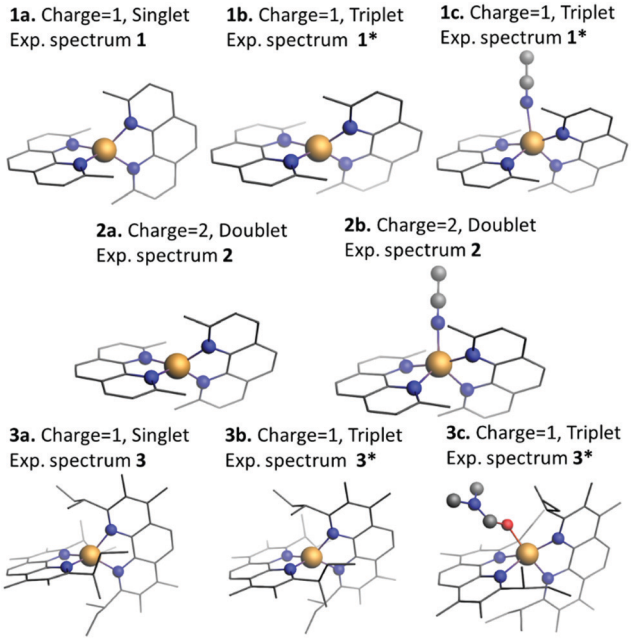

Fig. 4 Correspondence between different states of Cu complexes, experimental spectra and DFT models.

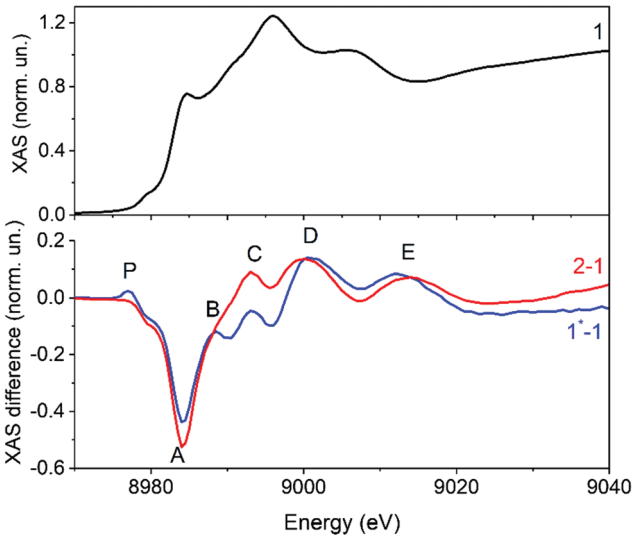

Fig. 5 Top: Experimental Cu K-edge XANES spectrum of $[Cu(dmp)_2]^+$ in the ground state. Bottom: The difference between electrochemically generated $[Cu(dmp)_2]^{2+}$ and the ground state of $[Cu(dmp)_2]^+$ (red line) and the difference between spectra of photoexcited triplet state and the ground state of $[Cu(dmp)_2]^+$ (blue line).

unlikely. To simplify the comparison between DFT models and experimental spectra discussed in the next sections we will use the notations summarized in Fig. 4.

Distinction between 4- and 5-coordinated Cu(II) states using XAS

Before addressing the question which structure is observed experimentally by transient X-ray absorption spectroscopy, we need to understand which features of the spectrum are sensitive to the formation of a five-coordinated structure when acetonitrile binds directly to the Cu(II) center. Insight can be obtained by comparing previously reported XANES spectra[19,28] of the photoexcited $[Cu(dmp)_2]^+$ MLCT state and electrochemically generated $[Cu^{II}(dmp)_2]^{2+}$ (**1*** and **2** from Fig. 4). If the structures of the Cu(II) complexes are identical, but the location of the electron which was removed from Cu is different (at the ligand for photoexcited MLCT state **1b** and not at the complex for **2a**) then the spectra are almost identical (Fig. S8, ESI†). Therefore dissimilarities between spectra of **1*** and **2** have a structural origin. To focus on the small spectral changes, we first show the differences between both spectra and **1**, the XANES of the ground state $[Cu(dmp)_2]^+$ (Fig. 5). The overall shapes of these spectra are similar with a strong negative peak A at 8984 eV that can be used to fingerprint the transition from Cu(I) to the Cu(II) state. Features D and E, which are above the main absorption maximum, originate from both structural changes of the complex and the overall shift of the spectrum induced by Cu oxidation. The main distinction between these two difference spectra is the absence of the pre-edge peak P and a more intense feature C (and less resolved peak B) in the electrochemically generated spectrum.

To understand changes in the pre-edge region, we performed a series of XANES simulations for Cu(II) structures ($[Cu^{II}(dmp)_2]^{2+}$ and $[Cu(dmp)_2]^+$ MLCT state) with different distances between Cu and acetonitrile. Fig. 6a demonstrates the comparison of the calculated spectrum for the 4-coordinated structure with the experimental pump–probe data. The ground-state contribution in the experimental excited-state spectrum has been removed as described previously.[28] Fig. 6b shows the pre-edge region of the XANES for different Cu–solvent distances. The intensity of the pre-edge peak P decreases as the Cu–acetonitrile distance decreases

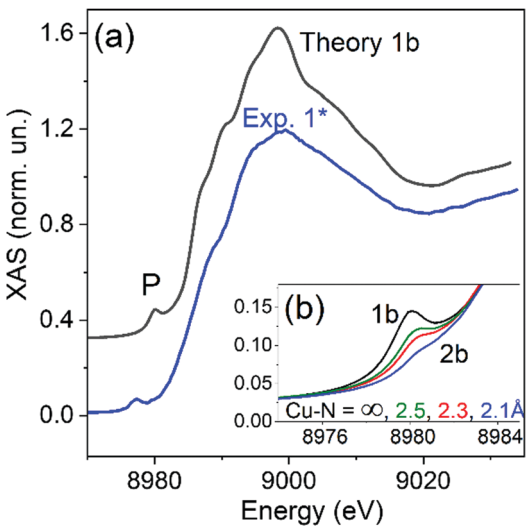

Fig. 6 (a) Calculated Cu K-edge XANES for the 4-coordinated model of triplet excited state of $[Cu(dmp)_2]^+$ in comparison with the spectrum from pump–probe experiment (b) calculations of the XANES pre-edge peak for the DFT optimized structure of the triplet state without solvent (black line), with an acetonitrile molecule fixed at 2.5 Å (green line), 2.3 Å (red line) and DFT optimized structure of $[Cu(dmp)_2]^{2+}$ which has a Cu–acetonitrile distance of 2.12 Å (blue line).

This journal is © the Owner Societies 2021

Published on 15 November 2021. Downloaded on 12/20/2021 11:28:06 AM.

and this spectral feature becomes weak for distances of less than 2.2 Å corresponding to the ligation. This effect is due to the lower mixing of Cu 3d and 4p states for 5-coordinated structures in comparison to 4-coordinated MLCT geometry (corresponding molecular orbitals are shown in Fig. S9 (ESI†) and the contributions of 3d and 4p states are summarized in Table S2, ESI†).

For further comparison of Cu(II) states, we show in Fig. 7 XANES calculations of the difference between the DFT-optimized five-coordinated Cu(II) structure and the four- coordinated structure of the triplet excited state. The outer shell of solvent molecules weakly influences the shape of the XANES spectrum (Fig. S10 and S11, ESI†) therefore it has been taken into account within the COSMO model.[33] The theoretical results are compared with the experimental difference between the spectra of electrochemically and photochemically generated Cu(II) states. The simulations reproduce not only the difference in the pre-edge region P but also the changes in the rising absorption edge region leading to shoulder C. Thus the absence of a pre-edge peak and rather high intensity of feature C (positive in the Cu(II)–Cu(I) difference spectrum, see Fig. 5) are indicators of the presence of a 5-coordinated Cu(II) structure.

The transient XANES for $[Cu(dmp)_2]^+$ in the triplet excited state reported in Fig. 5 and previous works[22,24,25] has a rather low intensity of feature C. The pre-edge feature P is also seen in a previous report[25] where the statistics was sufficient to distinguish this and therefore we can conclude that the observed photoexcited state is four-coordinated. Previously reported theoretical simulations[22] are somewhere between that of the spectra of the electrochemically generated Cu(II) reference and the spectrum of the photo-excited state. From the comparison of 4- and 5-coordinated Cu(II) models with the experimental data (Fig. 7) we see that the 5-coordinated model better describes the electrochemically generated structure than the photoexcited state.

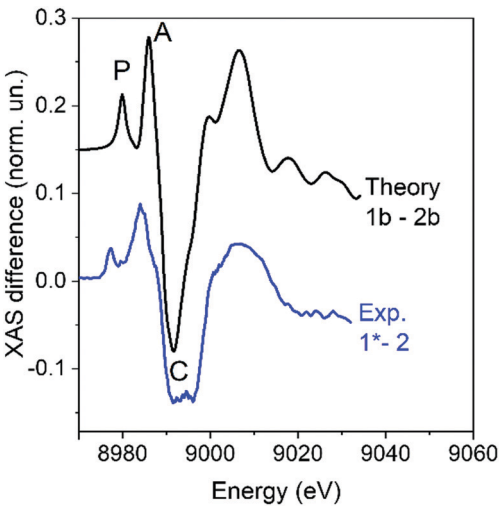

Fig. 7 Difference between experimental Cu(II) XANES of photoexcited $[Cu(dmp)_2]^+$ and electrochemically generated $[Cu(dmp)_2]^{2+}$ (blue line) is compared to the difference of theoretical spectra of Cu(II), corresponding to four-coordinated triplet state of $[Cu(dmp)_2]^+$ and five-coordinated DFT-optimized $[Cu(dmp)_2]^{2+}$ (black line).

Pump–probe XAS of $[Cu(dsbtmp)_2]^+$

The experimental transient XANES for $[Cu(dsbtmp)_2]^+$ obtained using the pump-sequential-probes method[34] is shown in Fig. 8. It has a clear pre-edge peak P and the intensity of feature C is negative which suggests a four-coordinated excited state structure. The overall shape of both ground state and transient spectra of $[Cu(dsbtmp)_2]^+$ and $[Cu(dmp)_2]^+$ are similar (Fig. S12, ESI†). Theoretical simulations of spectra for four-coordinated and five-coordinated excited state models, which are also shown in Fig. 8, confirm that the excited state is four-coordinated. Similar to $[Cu(dmp)_2]^+$ the intensity of feature C is too high for the five-coordinated structure. Moreover, the intensities of peaks D and E are underestimated. The theoretical spectrum of the four-coordinated model agrees with the experiment. The pre-edge peak is present only in the calculations for the four-coordinated structure; this feature is shifted by *ca.* 2 eV relative to the experiment due to the imperfections of the core hole screening. The excited-state lifetime for $[Cu(dsbtmp)_2]^+$ which we have measured using transient XANES (Fig. 8, right panel) is 1.01 ± 0.05 μs which is in reasonable agreement with transient optical measurements (1.3 μs).[20]

Discussion

For Cu-based complexes the spin–orbit coupling is rather small, and therefore the triplet excited state decay is mostly non-radiative with the rate described within the energy gap model.[26] Depending on the solvent polarity the electrostatic shielding of Cu complexes changes, which induces a

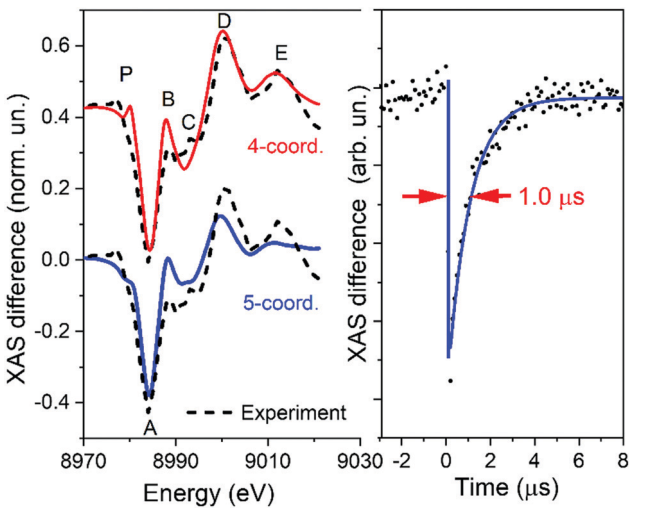

Fig. 8 Left panel: Experimental transient pump–probe XANES spectrum of $[Cu(dsbtmp)_2]^+$ in DMF (dashed lines) is compared with XANES calculations for DFT-optimized structures. The red line corresponds to 4-coordinated geometry of the triplet excited state with DMF solvation shell around the complex. The blue line corresponds to the 5-coordinated geometry of the triplet excited state, exciplex, with the $Cu–O_{DMF}$ distance 2.11 Å. Right panel: The experimental intensity of peak A of the transient XANES as a function of delay time between pump and probe (black dots) and exponential fit to these data (blue line).

Published on 15 November 2021. Downloaded on 12/20/2021 11:28:06 AM.

modification of the energy gap and corresponding changes of the excited state lifetime. To check the hypothesis that this effect alone can explain the solvent dependence of lifetimes observed, we have performed DFT calculations for two solvents, dichloromethane (DCM) and tetrahydrofuran (THF), which have different donating abilities (Gutmann's donor number is 1 kcal mol^{-1} for DCM and 20 kcal mol^{-1} for THF)[35] but similar polarity. The solvent was described within the COSMO model[33] to take into account the effect of electrostatic shielding only. The calculated energy gaps in these two solvents are similar (1.748 eV and 1.755 eV respectively) and according to the energy gap model should change the lifetime by $\sim$10% while the excited-state lifetimes reported in ref. 15 are significantly different: 90 ns in DCM and $<$10 ns in THF. Therefore, electrostatic shielding by the solvent is not the dominant factor influencing the excited state lifetime.

The formation of a short-lived exciplex, which has a short metal–solvent bond, cannot be excluded as a mechanism of the excited state decay. According to our DFT calculations, exciplex with a short metal–solvent bond is separated from the non-bound structure only by 0.24 eV. With a smaller energy gap (0.61 eV for the geometry of the exciplex with Cu–acetonitrile distance 2.15 Å in comparison to 1.25 eV for the four-coordinated structures) and significant structural difference between the ground and excited states, the rate of nonradiative decay is expected to be a few orders of magnitude higher for the exciplex.[36] Therefore even in the case of low probability to populate this state thermally it can influence on the overall decay of the excited state. Estimation of exciplex lifetime and the probability of interaction of solvent with the photoexcited complex can be obtained using quantum molecular dynamics or QM/MM for rather long, hundreds of nanoseconds, trajectories. For $[Cu(dmp)_2]^+$ QM/MM method was applied in the short time range ($\sim$10 ps) only.[25,31] The transition from a flattened structure to the exciplex with the short metal–solvent bond is energetically uphill and therefore slow in comparison to the decay of the exciplex, which explains why only the flattened four-coordinated structure is observed experimentally.

For $[Cu(dsbtmp)_2]^+$ the energy difference between the exciplex and the 4-coordinated triplet state is 0.73 eV, which makes a contribution of the decay of the exciplex state with any realistic speed irrelevant. Therefore, for $[Cu(dsbtmp)_2]^+$ the exciplex does not play a significant role in the excited state decay, which is in agreement with experimental data that the triplet excited state lifetime reduces in coordinating solvents not so significantly as in the case of $[Cu(dmp)_2]^+$ (by a factor of 1.9 in dichloromethane *versus* acetonitrile for $[Cu(dsbtmp)_2]^+$ and a factor of $\sim$56 for $[Cu(dmp)_2]^+$).[14,20] Observations reported in the literature that oxidation of $[Cu(dsbtmp)_2]^+$ at controlled potential electrolysis conditions is not fully reversible[15] indirectly confirms that Cu(II)–solvent interaction is possible even for this complex with bulky 2,9 substituents. Nevertheless, based on the combination of DFT and transient XANES results as presented here, we deduce that under photochemical conditions such interactions are significantly less probable for $[Cu(dsbtmp)_2]^+$ in comparison to $[Cu(dmp)_2]^+$.

Recently it has been observed that $-CH_2OCH_3$ and $-CH_2SCH_3$ substituents at 2,9 positions interact with Cu(II) center in the photoexcited state forming 5-coordinated complex[37] which could be explored as one of the strategies to develop photosensitizers. The interaction between the Cu(II) center and the solvent molecule could lead to quenching of the excited state and to degradation of the photosensitizer, which is unfavorable for its application. Nevertheless, this interaction also gives an opportunity to create photosensitizers with a long charge separation time using the supramolecular donor–acceptor strategy. If the electron moves rather far from the Cu donor to an acceptor, then a stable Cu(II) complex with the solvent can be formed that prevents charge recombination and further extends the lifetime of the charge-separated state.[38] Such an effect is probably observed for dyads with naphthalene-diimide acceptors linked to the Cu chromophore, where a complex with a phenanthroline group without any substituent at 2,9 positions has an order of magnitude longer charge-separated state lifetime than its analog with additional methyl groups at 2,9 positions.[12]

Methods

Experimental methods

Pump–probe XANES measurements at the Cu K-edge for $[Cu(dsbtmp)_2]^+$ have been performed at the SuperXAS beamline of the Swiss Light Source (SLS, Villigen, Switzerland). The storage ring was run in the top-up mode with an average current of 400 mA. The pump-sequential-probes XAS setup was used to acquire data in the asynchronous mode.[34] The X-ray beam was collimated by a Si-coated mirror at an incidence angle of 2.5 mrad, which also served for harmonic rejection. The energy has been scanned by a channel-cut Si(111) monochromator. A toroidal mirror with Rh coating was employed after the monochromator to focus the incident X-rays to a spot size of 100 $\times$ 100 μm^2. The photon flux at the sample was about 3×10^{11} photons pers. Excitation was performed at the second harmonic (395 nm) of a Wyvern 500 femtosecond laser amplifier (KM labs). The repetition rate of the laser was 50 kHz, with a pulse duration of $\sim$80 fs and the power at the sample position measured $\sim$0.7 W. The size of the laser spot at the sample was 300 $\times$ 220 μm^2. Approximately 70 mL of sample were circulated in the closed cycle flow system with laser and X-ray beams focused on the round jet of the sample with a diameter of 750 μm. This jet was placed in a chamber filled with N_2. The concentration of $[Cu(dsbtmp)_2]BF_4$ in anhydrous dimethylformamide solution was 1 mM. The solution was purged with N_2 for 30 minutes before optical and X-ray irradiation to remove dissolved oxygen and was kept in a N_2 atmosphere and continuously purged during the measurements. The synthesis of 2,9-di-*sec*-butyl-3,4,7,8-tetramethyl-1,10-phenanthroline (dsbtmp) and $[Cu(dsbtmp)_2]BF_4$ has been performed based on the reported procedure.[20] Details can be found in the ESI,† Fig. S1–S4. The Cu K-edge XANES data for $[Cu(dmp)_2]^+$ were reported previously[19,28] and were obtained at the Advanced Photon Source (APS) synchrotron, with the transient XANES data from the beamline 11ID-D.

 This journal is © the Owner Societies 2021

Published on 15 November 2021. Downloaded on 12/20/2021 11:28:06 AM.

The static XANES data for electrochemically generated $[Cu(II)(dmp)_2]^{2+}$ were obtained at the beamline 12BM as reported previously.[27] The monochromator with Si(111) crystals provided an energy resolution of around 1.3 eV. The design of the electrochemical cell was described in ref. 39. The oxidation was performed at 0.80 V potential measured *versus* an aqueous $Ag^+/AgCl$ reference electrode with platinum mesh used as the working electrode.

Theoretical methods

Geometry optimization, calculations of total energies and molecular orbitals were performed with ADF-2018 software[40,41] within density functional theory using B3LYP exchange–correlation functional[42] and large QZ4P basis set. Solvent effects were simulated employing the COSMO model with a dielectric medium around the molecule[33] and the validity of this approach is demonstrated in Fig. S10 and S11 of ESI† by considering explicit solvent molecules for spectrum simulation. Calculations for $[Cu(dsbtmp)_2]^+$ have been performed for two solvents, acetonitrile and DMF, for $[Cu(dmp)_2]^+$ we have used acetonitrile only. To study the interaction between photoexcited $[Cu(dmp)_2]^+$ complex and acetonitrile solvent we added an explicit CH_3CN molecule in the proximity of the Cu center, oriented by the N atom towards the metal. For some metal complexes, the interaction of ligands with solvent plays a major role in the photophysical processes, for example, due to the influence of metal-to-ligand π back-donation.[43] In such cases, explicit solvent molecules near ligands are necessary. Dmp and dsbtmp ligands are less active in this sense and only minor effects such as rotation of methyl groups of dmp[31] are expected from direct solvent-ligand interaction and they are induced by the solvent molecule which approaches the metal center. Therefore, only one solvent molecule which interacts with Cu has been used in the calculations explicitly. For each point shown in Fig. 3, the Cu–N distance was fixed while all atoms were allowed to relax their positions until variations of energy and atomic shifts were less than 1 meV and 0.01 Å. Such geometry optimization was performed for the triplet state and then total energies were calculated for the same structure in both singlet and triplet states. To allow direct comparison of models with and without additional acetonitrile molecule, as shown in Fig. 2, the bond energy of remote acetonitrile molecule was subtracted from the total bond energy of the corresponding structure with the additional solvent molecule.

Cu K-edge absorption spectra were obtained by calculating the transition probabilities between the core level and unoccupied molecular orbitals of the complex using numerical integration on a grid of points around the absorbing atom. Details of the procedure can be found in ref. 24 and 44. In general, 2000 orbitals were required to cover 50 eV energy range of the spectrum and both dipole and quadrupole matrix elements were taken into account. Self-consistent calculations were performed with unexcited core level and the chemical shift between singlet and triplet states was the result of the energy changes of 1s core level and unoccupied molecular orbitals. All theoretical spectra were shifted by a common value of energy to align the energy scale to the experimental one. To take into account the broadening of spectra due to core-hole lifetime, experimental resolution, and finite mean free path of the photoelectron a convolution of spectra was performed with a Lorentzian profile with energy-dependent width described by an arctangent function. The parameters of transition probabilities calculations (grid step and size, number of unoccupied molecular orbitals) and energy convolution were tested for convergence for the ground state and then fixed for all other models.

Conclusions

Both $[Cu(dmp)_2]^+$ and $[Cu(dsbtmp)_2]^+$ can form stable structures (corresponding to the local minimum of total energy) with a short bond between solvent and Cu of the complex in the triplet excited state as suggested by DFT calculations. For $[Cu(dsbtmp)_2]^+$ flattening is blocked, but solvent coordination is possible as a result of wagging distortions. While for $[Cu(dmp)_2]^+$ exciplex state with short Cu–solvent bond is not observed experimentally, 5-coordinated Cu(II) center is formed at electrochemical conditions. The excited-state decay through the exciplex state can explain the strong solvent dependence of the triplet lifetime for $[Cu(dmp)_2]^+$. The exciplex is not observed with pump–probe XANES because the transition from a four-coordinated to a five-coordinated geometry is likely much slower than the decay of the exciplex. For $[Cu(dsbtmp)_2]^+$ this decay mechanism plays a minor role due to the higher energy of the exciplex state and no sign of exciplex formation were found in the experimental pump–probe XANES data.

Conflicts of interest

There are no conflicts to declare.

Acknowledgements

We acknowledge the Paul Scherrer Institute, Villigen, Switzerland for the provision of beamtime at the SuperXAS beamline of the SLS. A. G. acknowledges financial support from Russian Foundation for Basic Research, project 18-02-40029. L. X. C. is supported by the U. S. Department of Energy, Office of Science, Office of Basic Energy Sciences, through Argonne National Laboratory under Contract No. DE-AC02-06CH11357. Furthermore, financial support from the University of Zürich, the University Research Priority Program LightChEC and the Swiss National Science Foundation (Grant CRSII2_160801/1) is acknowledged.

References

1 M. S. Lazorski and F. N. Castellano, *Polyhedron*, 2014, **82**, 57–70.
2 M. W. Mara, D. N. Bowman, O. Buyukcakir, M. L. Shelby, K. Haldrup, J. Huang, M. R. Harpham, A. B. Stickrath, X. Zhang, J. F. Stoddart, A. Coskun, E. Jakubikova and L. X. Chen, *J. Am. Chem. Soc.*, 2015, **137**, 9670–9684.

Published on 15 November 2021. Downloaded on 12/20/2021 11:28:06 AM.

3 B. Bozic-Weber, E. C. Constable and C. E. Housecroft, *Coord. Chem. Rev.*, 2013, **257**, 3089–3106.
4 C. E. Housecroft and E. C. Constable, *Chem. Soc. Rev.*, 2015, **44**, 8386–8398.
5 M. J. Leitl, D. M. Zink, A. Schinabeck, T. Baumann, D. Volz and H. Yersin, *Top. Curr. Chem.*, 2016, **374**, 25.
6 R. Czerwieniec, M. J. Leitl, H. H. H. Homeier and H. Yersin, *Coord. Chem. Rev.*, 2016, **325**, 2–28.
7 S.-P. Luo, E. Mejía, A. Friedrich, A. Pazidis, H. Junge, A.-E. Surkus, R. Jackstell, S. Denurra, S. Gladiali, S. Lochbrunner and M. Beller, *Angew. Chem., Int. Ed.*, 2013, **52**, 419–423.
8 E. Mejía, S.-P. Luo, M. Karnahl, A. Friedrich, S. Tschierlei, A.-E. Surkus, H. Junge, S. Gladiali, S. Lochbrunner and M. Beller, *Chem. – Eur. J.*, 2013, **19**, 15972–15978.
9 R. S. Khnayzer, C. E. McCusker, B. S. Olaiya and F. N. Castellano, *J. Am. Chem. Soc.*, 2013, **135**, 14068–14070.
10 J. Windisch, M. Orazietti, P. Hamm, R. Alberto and B. Probst, *ChemSusChem*, 2016, **9**, 1719–1726.
11 J. Huang, O. Buyukcakir, M. W. Mara, A. Coskun, N. M. Dimitrijevic, G. Barin, O. Kokhan, A. B. Stickrath, R. Ruppert, D. M. Tiede, J. F. Stoddart, J.-P. Sauvage and L. X. Chen, *Angew. Chem., Int. Ed.*, 2012, **51**, 12711–12715.
12 D. Hayes, L. Kohler, L. X. Chen and K. L. Mulfort, *J. Phys. Chem. Lett.*, 2018, **9**, 2070–2076.
13 D. Hayes, L. Kohler, R. G. Hadt, X. Zhang, C. Liu, K. L. Mulfort and L. X. Chen, *Chem. Sci.*, 2018, **9**, 860–875.
14 M. W. Mara, K. A. Fransted and L. X. Chen, *Coord. Chem. Rev.*, 2015, **282–283**, 2–18.
15 S. Garakyaraghi, E. O. Danilov, C. E. McCusker and F. N. Castellano, *J. Phys. Chem. A*, 2015, **119**, 3181–3193.
16 D. R. McMillin, J. R. Kirchhoff and K. V. Goodwin, *Coord. Chem. Rev.*, 1985, **64**, 83–92.
17 O. Horváth, *Coord. Chem. Rev.*, 1994, **135–136**, 303–324.
18 A. Horváth and K. L. Stevenson, *Coord. Chem. Rev.*, 1996, **153**, 57–82.
19 L. X. Chen, G. B. Shaw, I. Novozhilova, T. Liu, G. Jennings, K. Attenkofer, G. J. Meyer and P. Coppens, *J. Am. Chem. Soc.*, 2003, **125**, 7022–7034.
20 C. E. McCusker and F. N. Castellano, *Inorg. Chem.*, 2013, **52**, 8114–8120.
21 S. Garakyaraghi, P. D. Crapps, C. E. McCusker and F. N. Castellano, *Inorg. Chem.*, 2016, **55**, 10628–10636.
22 G. Smolentsev, A. V. Soldatov and L. X. Chen, *J. Phys. Chem. A*, 2008, **112**, 5363–5367.
23 S. P. Watton, *Acta Crystallogr., Sect. E: Struct. Rep. Online*, 2009, **65**, m585–m586.
24 M. Tromp, A. J. Dent, J. Headspith, T. L. Easun, X.-Z. Sun, M. W. George, O. Mathon, G. Smolentsev, M. L. Hamilton and J. Evans, *J. Phys. Chem. B*, 2013, **117**, 7381–7387.
25 T. J. Penfold, S. Karlsson, G. Capano, F. A. Lima, J. Rittmann, M. Reinhard, M. H. Rittmann-Frank, O. Braem, E. Baranoff, R. Abela, I. Tavernelli, U. Rothlisberger, C. J. Milne and M. Chergui, *J. Phys. Chem. A*, 2013, **117**, 4591–4601.
26 R. Englman and J. Jortner, *Mol. Phys.*, 1970, **18**, 145–164.
27 L. X. Chen, G. Jennings, T. Liu, D. J. Gosztola, J. P. Hessler, D. V. Scaltrito and G. J. Meyer, *J. Am. Chem. Soc.*, 2002, **124**, 10861–10867.
28 M. S. Kelley, M. L. Shelby, M. W. Mara, K. Haldrup, D. Hayes, R. G. Hadt, X. Zhang, A. B. Stickrath, R. Ruppert, J.-P. Sauvage, D. Zhu, H. T. Lemke, M. Chollet, G. C. Schatz and L. X. Chen, *J. Phys. B: At., Mol. Opt. Phys.*, 2017, **50**, 154006.
29 G. Capano, T. J. Penfold, M. Chergui and I. Tavernelli, *Phys. Chem. Chem. Phys.*, 2017, **19**, 19590–19600.
30 M. Iwamura, S. Takeuchi and T. Tahara, *Acc. Chem. Res.*, 2015, **48**, 782–791.
31 G. Levi, E. Biasin, A. O. Dohn and H. Jónsson, *Phys. Chem. Chem. Phys.*, 2020, **22**, 748–757.
32 V. Gutmann, *Coord. Chem. Rev.*, 1976, **18**, 225–255.
33 A. Klamt and G. Schüürmann, *J. Chem. Soc., Perkin Trans. 2*, 1993, 799–805.
34 G. Smolentsev, A. A. Guda, M. Janousch, C. Frieh, G. Jud, F. Zamponi, M. Chavarot-Kerlidou, V. Artero, J. A. van Bokhoven and M. Nachtegaal, *Faraday Discuss.*, 2014, **171**, 259–273.
35 C. Reichardt and T. Welton, *Solvents and Solvent Effects in Organic Chemistry*, John Wiley & Sons, Ltd, 4th edn, 2010.
36 K. F. Freed and J. Jortner, *J. Chem. Phys.*, 1970, **52**, 6272–6291.
37 M. Rentschler, S. Iglesias, M.-A. Schmid, C. Liu, S. Tschierlei, W. Frey, X. Zhang, M. Karnahl and D. Moonshiram, *Chem. – Eur. J.*, 2020, **26**, 9527–9536.
38 D. V. Scaltrito, C. A. Kelly, M. Ruthkosky, M. C. Zaros and G. J. Meyer, *Inorg. Chem.*, 2000, **39**, 3765–3770.
39 M. R. Antonio, L. Soderholm and I. Song, *J. Appl. Electrochem.*, 1997, **27**, 784–792.
40 C. F. Guerra, J. G. Snijders, G. te Velde and E. J. Baerends, *Theor. Chem. Acc.*, 1998, **99**, 391–403.
41 G. te Velde, F. M. Bickelhaupt, E. J. Baerends, C. Fonseca Guerra, S. J. A. van Gisbergen, J. G. Snijders and T. Ziegler, *J. Comput. Chem.*, 2001, **22**, 931–967.
42 M. Reiher, O. Salomon and B. Artur Hess, *Theor. Chem. Acc.*, 2001, **107**, 48–55.
43 K. S. Kjær, K. Kunnus, T. C. B. Harlang, T. B. V. Driel, K. Ledbetter, R. W. Hartsock, M. E. Reinhard, S. Koroidov, L. Li, M. G. Laursen, E. Biasin, F. B. Hansen, P. Vester, M. Christensen, K. Haldrup, M. M. Nielsen, P. Chabera, Y. Liu, H. Tatsuno, C. Timm, J. Uhlig, V. Sundström, Z. Németh, D. S. Szemes, É. Bajnóczi, G. Vankó, R. Alonso-Mori, J. M. Glownia, S. Nelson, M. Sikorski, D. Sokaras, H. T. Lemke, S. E. Canton, K. Wärnmark, P. Persson, A. A. Cordones and K. J. Gaffney, *Phys. Chem. Chem. Phys.*, 2018, **20**, 4238–4249.
44 I. Alperovich, G. Smolentsev, D. Moonshiram, J. W. Jurss, J. J. Concepcion, T. J. Meyer, A. Soldatov and Y. Pushkar, *J. Am. Chem. Soc.*, 2011, **133**, 15786–15794.

 This journal is © the Owner Societies 2021